iScience

CellPress
OPEN ACCESS

Article

Image-based deep learning model to predict stoma-site incisional hernia in patients with temporary ileostomy: A retrospective study

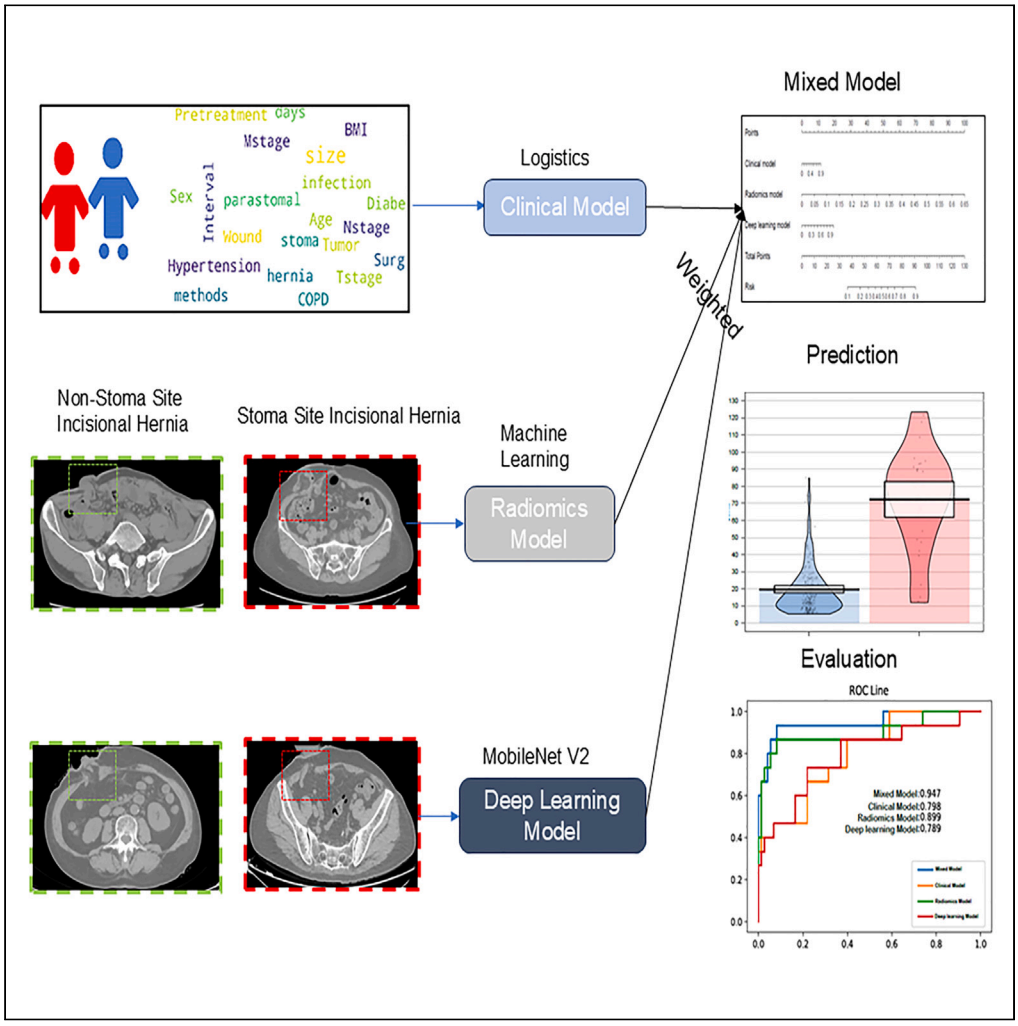

Zhongyi Dong, Jianhua Cai, Haigang Geng, ..., Yan Gu, Hui Cao, Zizhen Zhang

yangu@shsmu.edu.cn (Y.G.)
caohui@renji.com (H.C.)
zhangzizhen@renji.com (Z.Z.)

Highlights

We developed a mixed model to predict SSIH based on the patient's preoperative CT images

The model also achieved great predictive efficiency in non-tumor patients with stoma

It is the first study to use deep learning for the prediction of hernia occurrence

Dong et al., iScience 27, 111235
November 15, 2024
https://doi.org/10.1016/j.isci.2024.111235

iScience

CellPress
OPEN ACCESS

Article

Image-based deep learning model to predict stoma-site incisional hernia in patients with temporary ileostomy: A retrospective study

Zhongyi Dong,[1,6] Jianhua Cai,[2,6] Haigang Geng,[1,6] Bo Ni,[1,6] Mengqing Yuan,[3] Yeqian Zhang,[1] Xiang Xia,[1] Haoyu Zhang,[1] Jie Zhang,[4] Chunchao Zhu,[1] Un Wai Choi,[5] Aksara Regmi,[5] Cheok I. Chan,[5] Cara Kou Yan,[5] Yan Gu,[2,*] Hui Cao,[1,*] and Zizhen Zhang[1,7,*]

SUMMARY

The prophylactic implantation of biological mesh can effectively prevent the occurrence of stoma-site incisional hernia (SSIH) in patients undergoing stoma retraction. Therefore, our study prospectively established and validated a mixed model, which combined radiomics, stepwise regression, and deep learning for the prediction of SSIH in patients with temporary ileostomy. The mixed model showed good discrimination of the SSIH patients on all cohorts, which outperformed deep learning, radiomics, and clinical models alone (overall area under the curve [AUC]: 0.947 in the primary cohort, 0.876 in the external validation cohort 1, and 0.776 in the external validation cohort 2). Moreover, the sensitivity, specificity, and precision for predicting SSIH were improved in the mixed model. Thus, the mixed model can provide more information for SSIH precaution and clinical decision-making.

INTRODUCTION

Colorectal cancer is the third most common cancer and second leading cause of cancer-related deaths worldwide.[1] With the development of enteroscopic and imaging screening technologies, detection rates of early-stage colorectal cancer have improved.[2] Meanwhile, laparoscopic and robotic surgical techniques have made it more feasible to perform one-stage procedures involving primary anastomosis and sphincter-preserving surgery for patients with low and ultra-low rectal cancer. Temporary ileostomy is a classic surgical procedure performed to prevent anastomotic leakage after bowel resection.[3] Although its benefits include reduced rates of surgical site infection and rapid recovery of intestinal function, it also inevitably disturbs abdominal wall integrity and disrupts the tension balance.[4] Abdominal wall defects resulting from ostomy or stoma reduction procedures pose a significant challenge for gastrointestinal surgeons because of the high likelihood of stoma-site incisional hernia (SSIH) development.[5] SSIH can cause clinical symptoms, such as regional pain, abdominal mass, hernia content incarceration, intestinal obstruction, and other potential complications, which have a significant impact on a patient's quality of life and self-image.[6] To address these issues, more than 35% of the patients undergo incisional hernia repair surgery.[4] To avoid additional stigma caused by reoperation, the Reinforcement of Closure of Stoma Site (ROCSS) collaborative attempted to perform prophylactic biological mesh reinforcement, which has produced satisfactory results.[7] In addition, other preventive measures such as enhancing nutrition after stoma closure, reducing the risk of infection, long-term use of abdominal bands, weight control, and avoiding heavy lifting to reduce intra-abdominal pressure can effectively reduce the incidence of SSIH. Therefore, it is crucial for surgeons to identify patients with high-risk SSIH based on their preoperative features and implement interventions as necessary.

Radiomics is an emerging technique for quantifying region of interest (ROI) characteristics with high-throughput radiomic features and has been categorized into two main groups: handcrafted and deep learning-based radiomics.[8] It has been widely used and has shown promising results in personalized diagnosis and treatment of patients with tumors. At present, the mixed model, which combines the radiomic signature and clinical characteristics, has greatly improved predictive power.[9] However, its application in the field of postoperative complications is still lacking, and the use of deep learning radiomics to predict SSIHs has yet to be reported.

In this study, we attempted to use radiomics to identify patients who are at high risk of SSIH by constructing a mixed model and evaluating its performance through internal and external validation sets. Thus, based on the prediction results, surgeons can pre-implant a biological mesh to reduce the risk of herniation in at-risk patients.

[1]Department of Gastrointestinal Surgery, Renji Hospital, School of Medicine, Shanghai Jiaotong University, Shanghai 200127, P.R. China
[2]Department of General Surgery, Fudan University Affiliated Huadong Hospital, Shanghai 200040, P.R. China
[3]School of Science, The Hongkong University of Science and Technology, Hongkong 999077, P.R. China
[4]Department of Interventional Oncology, Renji Hospital, School of Medicine, Shanghai Jiaotong University, Shanghai 200127, P.R. China
[5]School of Medicine, Shanghai Jiaotong University, Shanghai 200025, P.R. China
[6]These authors contributed equally
[7]Lead contact
*Correspondence: yangu@shsmu.edu.cn (Y.G.), caohui@renji.com (H.C.), zhangzizhen@renji.com (Z.Z.)
https://doi.org/10.1016/j.isci.2024.111235

Table 1. Clinical characteristics of Renji cohort and external cohort 1

	Renji cohort			Huadong cohort		
Characteristic	No-SSIH	SSIH	*p* value	No-SSIH	SSIH	*p* value
Age						
≤65	112 (60.22%)	13 (38.24%)	0.017	17 (43.59%)	3 (50.00%)	0.769
>65	74 (39.78%)	21 (61.76%)		22 (56.41%)	3 (50.00%)	
Sex						
Male	120 (64.52%)	23 (67.65%)	0.725	23 (58.97%)	3 (50.00%)	0.679
Female	66 (35.48%)	11 (32.35%)		16 (41.03%)	3 (50.00%)	
Parastomal hernia						
Yes	15 (8.06%)	12 (35.29%)	<0.001	6 (15.38%)	3 (50.00%)	0.048
No	171 (91.94%)	22 (64.71%)		33 (84.62%)	3 (50.00%)	
Tumor size						
≤45 mm	119 (63.98%)	22 (64.71%)	0.935	25 (64.10%)	3 (50.00%)	0.507
>45 mm	67 (36.02%)	12 (35.29%)		14 (35.90%)	3 (50.00%)	
Tumor distance from anal margin						
<7 cm	108 (58.06%)	12 (35.29%)	0.014	18 (46.15%)	4 (66.67%)	0.349
≥7 cm	78 (41.94%)	22 (64.71%)		21 (53.85%)	2 (33.33%)	
Surgical methods						
Laparoscopic	158 (84.95%)	27 (79.41%)	0.417	28 (71.79%)	5 (83.33%)	0.552
Open surgery	28 (15.05%)	7 (20.59%)		11 (28.21%)	1 (16.67%)	
T stage						
T1	19 (10.22%)	5 (14.71%)	0.761	3 (7.69%)	1 (16.67%)	0.832
T2	37 (19.89%)	5 (14.71%)		10 (25.64%)	3 (50.00%)	
T3	50 (26.88%)	8 (23.53%)		22 (56.41%)	1 (16.67%)	
T4	80 (43.01%)	16 (47.05%)		4 (10.26%)	1 (16.67%)	
N stage						
N0	102 (54.84%)	21 (61.76%)	0.745	21 (53.85%)	3 (50.00%)	0.390
N1	56 (30.11%)	9 (26.47%)		5 (12.82%)	2 (33.33%)	
N2	28 (12.36%)	4 (11.43%)		13 (33.33%)	1 (16.67%)	
M stage						
M0	176 (94.62%)	31 (91.18%)	0.433	37 (94.87%)	5 (83.33%)	0.292
M1	10 (5.38%)	3 (8.82%)		2 (5.13%)	1 (16.67%)	
BMI						
≤24 kg/m^2	137 (73.66%)	18 (52.94%)	0.015	26 (66.67%)	2 (33.33%)	0.117
>24 kg/m^2	49 (26.34%)	16 (47.06%)		13 (33.33%)	4 (66.67%)	
Pre-chemotherapy						
Yes	94 (50.54%)	22 (64.71%)	0.128	29 (74.36%)	2 (33.33%)	0.043
No	92 (49.46%)	12 (35.29%)		10 (25.64%)	4 (66.67%)	
Pre-albumin						
<40 g/L	76 (40.86%)	10 (29.41%)	0.208	25 (64.10%)	2 (33.33%)	0.152
≥40 g/L	110 (59.14%)	24 (70.59%)		14 (35.90%)	4 (66.67%)	
Wound infection						
Yes	166 (89.25%)	27 (79.41%)	0.108	36 (92.31%)	6 (100.00%)	0.482
No	20 (10.75%)	7 (20.59%)		3 (7.69%)	0 (0.00%)	

(*Continued on next page*)

Table 1. *Continued*

Characteristic	Renji cohort			Huadong cohort		
	No-SSIH	SSIH	*p* value	No-SSIH	SSIH	*p* value
Stoma period						
≤6 months	83 (44.62%)	9 (26.47%)	0.048	28 (71.79%)	3 (33.33%)	0.283
>6 months	103 (55.38%)	25 (73.53%)		11 (28.21%)	3 (66.67%)	
Hypertension						
Yes	48 (25.81%)	12 (35.29%)	0.253	10 (25.64%)	0 (0.00%)	0.160
No	138 (74.19%)	22 (64.71%)		29 (74.36%)	6 (100.00%)	
Diabetes						
Yes	25 (13.44%)	4 (11.76%)	0.791	4 (9.30%)	1 (11.11%)	0.642
No	161 (86.56%)	30 (88.24%)		35 (90.70%)	5 (88.89%)	
COPD						
Yes	11 (5.91%)	19 (55.88%)	<0.001	0 (0.00%)	1 (11.11%)	0.010
No	175 (94.09%)	15 (44.12%)		39 (100.00%)	5 (88.89%)	
Stoma size						
≤25 mm	125 (67.20%)	22 (64.71%)	0.776	15 (39.53%)	1 (22.22%)	0.299
>25 mm	61 (32.80%)	12 (35.29%)		24 (60.47%)	5 (77.78%)	
Trans or lateral rectus abdominis (stoma)						
Trans	92 (49.46%)	22 (64.71%)	0.102	20 (51.16%)	3 (44.44%)	0.953
Lateral	94 (50.54%)	12 (35.29%)		19 (48.84%)	3 (55.56%)	

RESULTS

Clinical characteristics

The detailed clinicopathological characteristics of the patients and SSIH outcomes in the primary cohort (n = 220) and external cohort 1 (n = 45) are listed in Table 1. The flow of patient inclusion is displayed in Figure 1. The incidence of SSIH one year after the closure was 15.5% (Renji Cohort) and 13.3% (Huadong Cohort), respectively. Chi-squared tests showed that the two cohorts from different institutions had similar and well-balanced characteristics. Correlations between clinical features are shown in Figure S1A. Based on the stepwise regression analysis, we identified five variables in the best clinical model. High-risk SSIH was significantly associated with larger stoma size, older age, parastomal hernia, pre-chemotherapy, and chronic obstructive pulmonary disease (COPD).

Radiomics feature selection and signature building

After assessing the reproducibility (inter-class correlation coefficient [ICC] > 0.75) and correlations (R < 0.90), 1,255 features from soft tissue (ROI-1) and 1,170 features from muscle (ROI-2) were selected. Bar diagrams are shown in Figure S1B. We then integrated the radiomics features of muscle and soft tissue into a comprehensive model and employed least absolute shrinkage and selection operator (LASSO) regression to evaluate the features correlated with SSIH (Figures S2A and S2B). The top 10 ranking features are shown in Figure S2C. To avoid overfitting, we constructed a radiomics model with features whose absolute coefficient values were greater than 0.015 (Table S2). The radiomics characteristics of both categories are shown in Figure S3.

Three different types of supervised learning methods were used in the construction of the radiomics model: support vector machine (SVM), random forest (RF), and an artificial neural network (ANN). In 10 cross-validations, all models had similar area under the curve (AUC) (Figures S4A and S4B). Then, we developed an ensemble model by combining the three models based on their respective weights. The Kolmogorov-Smirnov test, which was used for model optimization, defined the optimal threshold as 0.231. The Kolmogorov-Smirnov (KS) value was 0.61, revealing good discrimination ability of the model (Figure S4C). Finally, a confusion matrix was constructed to assess the performance of the mixed model (Figure S4D). This suggests that the radiomic model has high specificity (64/73, 0.877) and modest sensitivity (10/15, 0.667). However, the precision was unsatisfactory (10/19, 0.526).

Deep learning model construction

Considering the limited number of cases in our study, we eventually used the lightweight convolutional neural network MobileNetV2 for transfer learning. The deep learning model showed good accuracy, with an AUC of 0.748 (95% confidence interval [CI] = 0.613–0.870) and a KS value of 0.499, suggesting good predictive power (Figures S5A and S5B). The confusion matrix shows that although this model

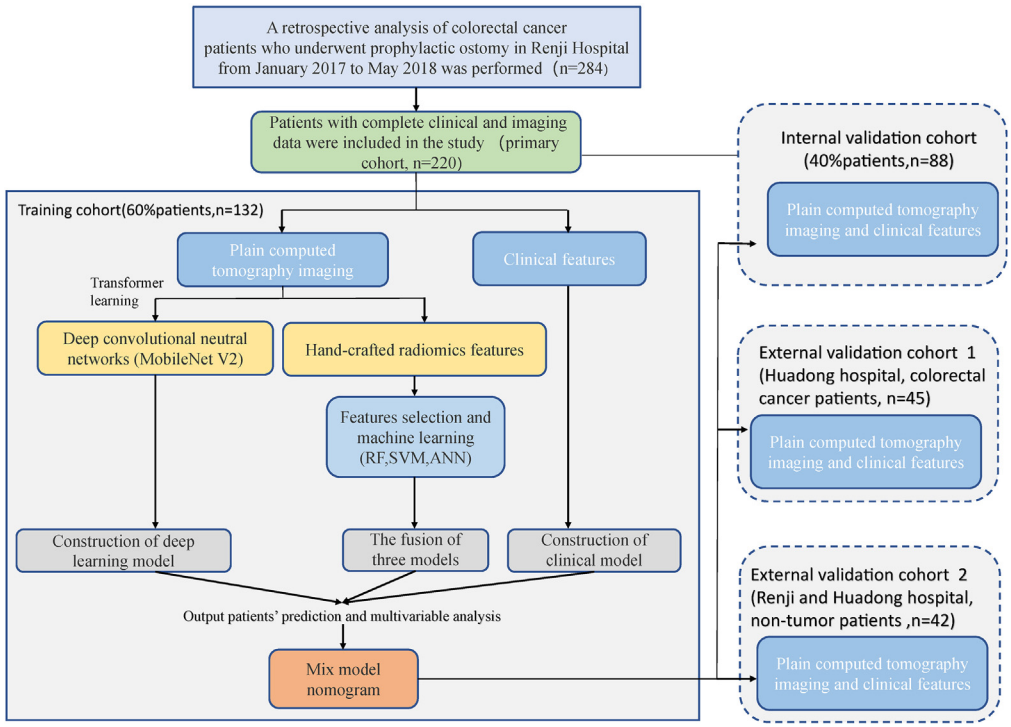

Figure 1. Flowchart of this multi-cohort study

has high specificity (51/73, 0.699) and sensitivity (11/15, 0.733) after adjusting for the best threshold using the Kolmogorov-Smirnov test, it still has some shortcomings in terms of precision (11/33, 0.333) (Figure S5C). The class activation maps of the four patients are shown in Figures S5D and S5E. We can intuitively observe that the soft tissue and muscle sections of patients have higher intensities than those of patients without SSIH.

Mixed model construction and validation

The workflow of mixed model construction and validation is illustrated in Figure 2. Logistic regression was performed based on the prediction results from clinical, radiomics, and deep learning models, and the final nomogram was built (Figure 3A). The risk score distribution was significantly different between the two groups in both the internal and external validation cohort 1 (Figures 3B, 3C, and 3H). The mixed model not only achieved a maximum AUC of 0.947 (95% CI = 0.850–0.997) but also showed the best discriminating ability in the Kolmogorov-Smirnov test (Figures 3D and 3E). The KS value of the mixed model was 0.851, which means that it performed much better than the radiomics (0.610) and deep learning models (0.499). The confusion matrix revealed that the model had high specificity (67/73, 0.918) and sensitivity (13/15, 0.867). Furthermore, the precision (13/19, 0.684) showed a distinct improvement (Figure 3G). Based on the DeLong test, the mixed model showed a significantly higher AUC than the clinical and deep learning models (Table S3). Because we adjusted the threshold of the mixed model according to the Kolmogorov-Smirnov test, the calibration curve was no longer suitable for evaluation. We could only implement decision curve analysis (DCA) to compare the clinical availability and benefits of all models (Figure 3F). This reveals the net benefit of different threshold probabilities. Fortunately, the best performances of the three models were achieved at different threshold ranges (Radiomics Model (RM): 0–0.5, Deep learning Model (DM): 0.5–0.7, Clinical Model (CM): 0.7–1). When the three models are merged into a mixed model, it made significant gains in each point.

Based on the results derived from the training set, we noted that the features required for this model were independent of the tumor condition. Therefore, we considered whether the model could be extended to non-tumor patients. We further validated our mixed model in two external validation cohorts: external validation cohort 1, which consisted of patients with colorectal cancer (CRC) from Huadong Hospital (Table 1), and external validation cohort 2, which consisted of non-tumor patients (Table S1). Surprisingly, the mixed model achieved a high AUC in both patients with CRC (Figure 3I) and non-tumor patients (Figure S6B). However, the precision remained high (Figures 3J and S6C).

DISCUSSION

In this retrospective study, we developed and validated a mixed model that combines clinical features, radiomics, and deep learning to accurately predict SSIH based on preoperative computed tomography (CT) images. Patients who undergo temporary ileostomy are often at increased risk of developing complications such as incisional hernia formation after abdominal stoma closure.[7] Accurate prediction of

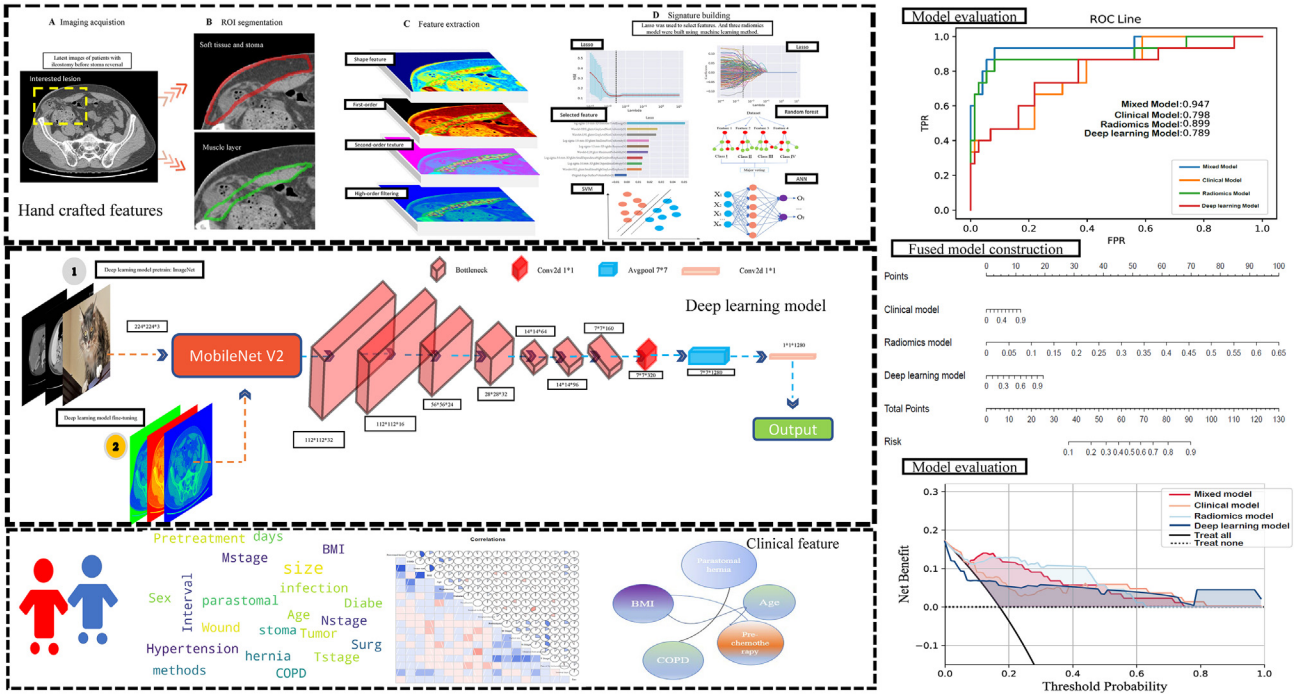

Figure 2. Workflow of mixed modeling for predicting SSIH in temporary ileostomy patients

SSIH before stoma closure is crucial for timely prevention measures such as prophylactic biological mesh reinforcement. Therefore, we constructed a nomogram as an easy-to-use, preoperative, and individualized diagnostic tool for SSIH.

The development of incisional hernia is an early complication of classical laparotomy,[10] and the rate of incisional hernia increases with longer follow-up.[11] Lambrichts et al. conducted a meta-analysis of 33 clinical studies involving patients with SSIH after stoma closure.[12] The study included 4,679 patients, among whom the overall rate of SSIH was 6.5%. Another study revealed that the combined clinical and radiological SSIH rate was 34% (20/59), with a median time from closure to imaging of 10 months. Notably, imaging alone produced a detection rate of 31% (18/59), which was significantly higher than the clinical hernia detection rate of 14% (8/59).[13] In this study, we combined physical examinations and CT scans within one year to assess the presence or absence of SSIH in the patient population.

In patients with colon cancer, the situation regarding SSIH is complex. Prophylactic colostomy for colorectal cancer can cause a local tissue defect in the abdominal wall, and stoma closure often involves a spindle-shaped incision, which means that a portion of the tissue around the stoma must be removed, inevitably resulting in fascial defects and excessive suture tension. Moreover, incisions in these patients are susceptible to hematoma, infection, or poor healing.[14] Postoperative abdominal bloating, elevated intra-abdominal pressure, enteritis, and intestinal dysbacteriosis caused by chemotherapy and radiotherapy are significant risk factors for SSIH.[15] Elective incisional hernia repair is the most efficient way to achieve a complete cure. However, for patients with colon cancer, surgeons must consider the additional risks of recurrence and metastasis associated with SSIH. Therefore, the best treatment for these patients is the prevention of SSIH. Fortunately, prophylactic implantation of a biological mesh during stoma closure can significantly reduce the incidence of SSIH.[7] Although it may take longer to perform this procedure during surgery, complications such as seroma, anastomotic leakage, and length of hospital stay did not significantly differ. On the other hand, implementing this procedure universally for all patients may escalate healthcare expenses and elevate the likelihood of surgical site infections. Especially for patients with colorectal cancer, undergoing numerous surgeries within a brief time frame could potentially influence the progression of the tumor. The impact of using biological patches on patients' relapse-free survival rates and the potential increase in peritoneal metastasis risk remains to be further studied. Therefore, it is imperative to screen potentially high-risk populations for appropriate precision medicine treatments.

Our mixed model has the potential to assist gastrointestinal surgeons in selecting patients suitable for appropriate preventive measures. Moreover, DCA demonstrated that using our mixed model to guide prophylactic mesh implantation could significantly benefit patients compared to both non-implantation and all-implantation schemes. This study was performed on two ROIs from a single CT image rather than combining muscle and soft tissues into one ROI. After using LASSO regression analysis to shrink the SSIH candidates, the radiomic features extracted from the soft tissues were preserved. This suggests that preoperative soft tissue conditions should be carefully considered for these patients, instead of focusing solely on abdominal wall muscle defects. It is evident why the "first-order" in soft tissue features plays a great role in analysis as abdominal fat thickness is closely related to BMI, which is an essential risk factor for SSIH.[16] Additionally, peristomal infection, adjacent soft tissue edema, and inadequate blood supply at the surgical site may increase the risk of SSIH. Although we cannot

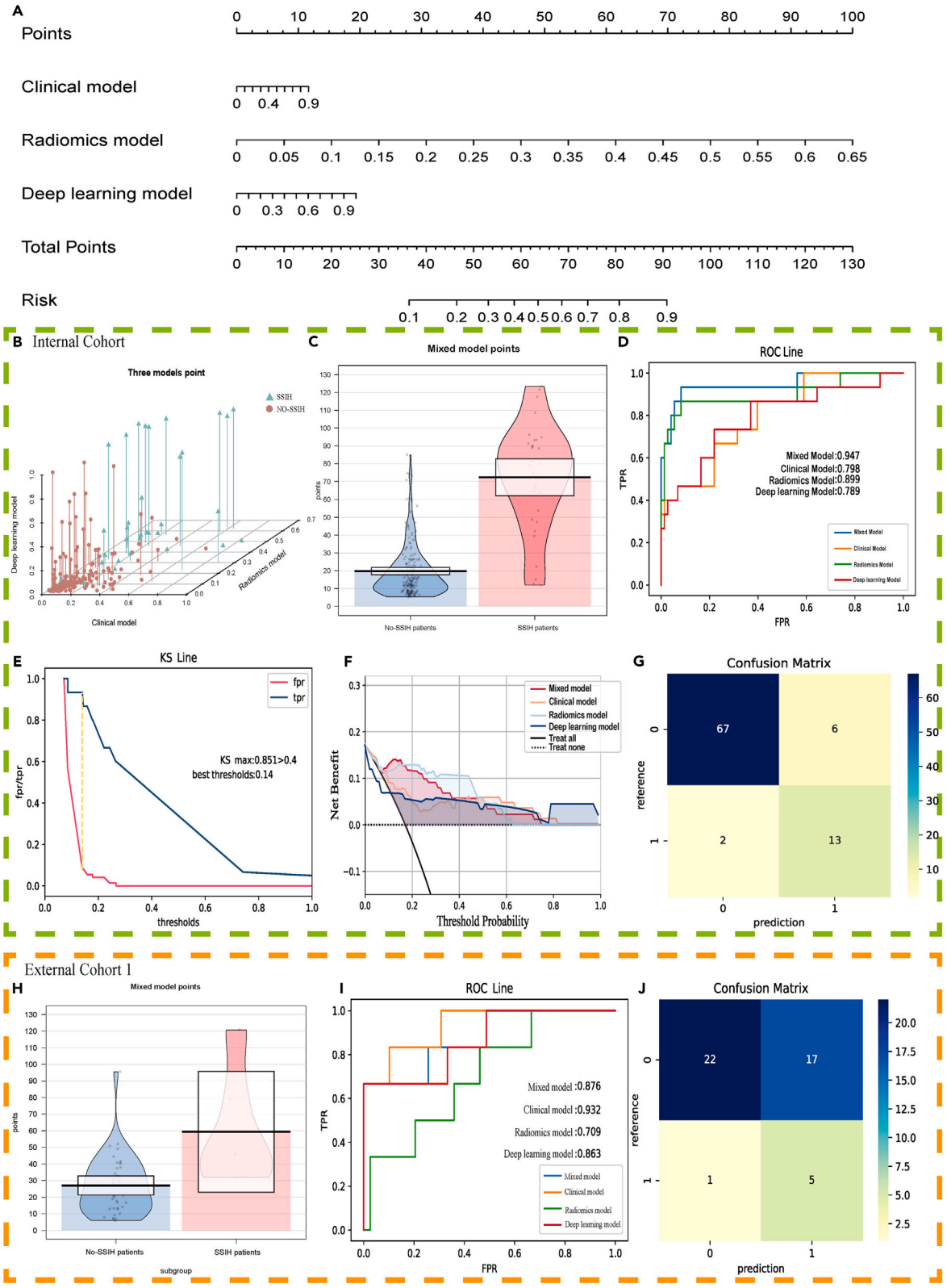
A
Points
Clinical model
Radiomics model
Deep learning model
Total Points
Risk
B Internal Cohort
Three models point
SSIH
NO-SSIH
Deep learning model
Radiomics model
Clinical model
C
Mixed model points
points
No-SSIH patients
SSIH patients
D
ROC Line
TPR
FPR
Mixed Model:0.947
Clinical Model:0.798
Radiomics Model:0.899
Deep learning Model:0.789
Mixed Model
Clinical Model
Radiomics Model
Deep learning Model
E
KS Line
fpr
tpr
fpr/tpr
KS max:0.851>0.4
best thresholds:0.14
thresholds
F
Mixed model
Clinical model
Radiomics model
Deep learning model
Treat all
Treat none
Net Benefit
Threshold Probability
G
Confusion Matrix
67
6
2
13
reference
prediction
External Cohort 1
H
Mixed model points
points
No-SSIH patients
SSIH patients
subgroup
I
ROC Line
TPR
FPR
Mixed model :0.876
Clinical model :0.932
Radiomics model :0.709
Deep learning model :0.863
Mixed model
Clinical model
Radiomics model
Deep learning model
J
Confusion Matrix
22
17
1
5
reference
prediction

Figure 3. Mixed model and its performance

(A) Mixed nomogram with clinical model, radiomics model, and deep learning model. The points of three independent models are obtained based on the top "points" bar with scale of 0–100. Then, the mixed model will output a predicted probability based on the final point, which is calculated by summing the three points.

(B) Three-dimensional point plots show the scores of the two types of patients according to three different model assessments.

(C) The pirate plot shows the scores of the mixed model for the two subgroups.

(D) AUC curve of four prediction models.

(E) The KS curve is used to assess the risk-differentiation ability of the mixed model.

(F) Decision curve analysis for guiding prophylactic patch implantation using the mixed model, clinical, radiomics, deep learning model, none-implantation, and all-implantation scheme.

(G) The mixed model confusion matrix.

(H) The pirate plot in external cohort 1.

(I) AUC curve of four prediction models in external cohort 1.

(J) The external cohort 1 confusion matrix.

directly establish a relationship between a specific imaging feature and these factors, radiomics can capture the differences caused by them through gray-level changes in CT images.

We believe that imaging can be used not only for the analysis of tumor tissues but also for the prediction of complications in non-tumor patients. At present, most radiomics researchers still focus on the tumor area as ROIs; however, we believe that it can play a more important role.

Limitations of the study

In general, our model achieved excellent performance. However, this study has some limitations. First, the sample size of the study, particularly for patients with SSIH, was relatively small, which may have affected the precision and sensitivity of our model to some extent. Further prospective studies involving large populations are warranted. Second, although the enrolled patients were treated with standard and homogenized treatments, there may have been differences between the procedures performed by different surgeons. Third, we used 2D features from a single slice rather than 3D features. However, some researchers have reported that better reliability performed on 2D images than on 3D images may limit the representativeness of the entire stoma and potentially affect some features.[17] Finally, although our model performed well in non-tumor patients, its precision could still be improved, suggesting that there may be remaining high-risk factors that were not considered.

Conclusions

In conclusion, a mixed nomogram had good predictive ability for SSIH in patients with temporary ileostomy, which could provide basic information for individual diagnosis and treatment.

RESOURCE AVAILABILITY

Lead contact

Further information and requests for resources should be directed to and will be fulfilled by the lead contact, Zizhen Zhang (zhangzizhen@renji.com).

Materials availability

This study did not generate new unique reagents.

Data and code availability

- The data governed by Renji and Huadong Hospital are not publicly shared but can be made available upon reasonable request from the lead contact.
- All original code has been deposited at Mendeley Data and is publicly available as of the date of publication. DOIs are listed in the key resources table.
- Any additional information required to reanalyze the data reported in this paper is available from the lead contact upon request.

ACKNOWLEDGMENTS

The authors would like to thank all the reviewers who participated in the review.

Z.Z. is supported by the National Natural Science Foundation of China (grant numbers: 81972206 and 82173215).

AUTHOR CONTRIBUTIONS

Z.Z., H.C., and Y.G. conceived and designed the study. B.N., Y.Z., U.W.C., A.R., C.I.C., X.X., C.Z., J.Z., and C.K.Y. acquired the data. Z.D., J.C., and H.G. did the statistical analyses. Z.D., H.G., and M.Y. developed, trained, and applied the artificial intelligence model. J.Z., C.Z., X.X., and C.I.C. implemented quality control of data and the algorithms. U.W.C., A.R., C.I.C., and Y.Z. verified the underlying raw data. All authors had access to the data presented in the manuscript. All authors analyzed and interpreted the data. Z.D., J.Z., and H.G. prepared the first draft of the manuscript. Z.Z., H.C., and Y.G. revised the manuscript. All authors contributed to manuscript preparation. All authors were responsible for the decision to submit the manuscript for publication.

DECLARATION OF INTERESTS

The authors declare no competing interests.

STAR★METHODS

Detailed methods are provided in the online version of this paper and include the following:

- KEY RESOURCES TABLE
- EXPERIMENTAL MODEL AND STUDY PARTICIPANT DETAILS
- METHOD DETAILS
  - Patients and datasets
  - Radiomics and clinical features extraction
  - Architecture of radiomics models
  - Deep learning image processing
  - Models
- QUANTIFICATION AND STATISTICAL ANALYSIS

SUPPLEMENTAL INFORMATION

Supplemental information can be found online at https://doi.org/10.1016/j.isci.2024.111235.

Received: January 22, 2024
Revised: May 22, 2024
Accepted: October 21, 2024
Published: October 22, 2024

REFERENCES

1. Sung, H., Ferlay, J., Siegel, R.L., Laversanne, M., Soerjomataram, I., Jemal, A., and Bray, F. (2021). Global cancer statistics 2020: GLOBOCAN estimates of incidence and mortality worldwide for 36 cancers in 185 countries. CA Cancer J Clin *71*, 209–249.
2. Lee, H.L., Eun, C.S., Lee, O.Y., Han, D.S., Yoon, B.C., Choi, H.S., Hahm, J.S., and Koh, D.H. (2010). When do we miss synchronous gastric neoplasms with endoscopy? Gastrointest. Endosc. *71*, 1159–1165.
3. Montedori, A., Cirocchi, R., Farinella, E., Sciannameo, F., and Abraha, I. (2010). Covering ileo- or colostomy in anterior resection for rectal carcinoma. Cochrane Database Syst. Rev. CD006878.
4. Bhangu, A., Nepogodiev, D., and Futaba, K.; West Midlands Research Collaborative (2012). Systematic review and meta-analysis of the incidence of incisional hernia at the site of stoma closure. World J. Surg. *36*, 973–983.
5. Peltrini, R., Imperatore, N., Altieri, G., Castiglioni, S., Di Nuzzo, M.M., Grimaldi, L., D'Ambra, M., Lionetti, R., Bracale, U., and Corcione, F. (2021). Prevention of incisional hernia at the site of stoma closure with different reinforcing mesh types: a systematic review and meta-analysis. Hernia *25*, 639–648.
6. van Ramshorst, G.H., Eker, H.H., Hop, W.C.J., Jeekel, J., and Lange, J.F. (2012). Impact of incisional hernia on health-related quality of life and body image: a prospective cohort study. Am. J. Surg. *204*, 144–150.
7. Reinforcement of Closure of Stoma Site C, West Midlands Research C (2020). Prophylactic biological mesh reinforcement versus standard closure of stoma site (ROCSS): a multicentre, randomised controlled trial. Lancet *395*, 417–426.
8. Lambin, P., Leijenaar, R.T.H., Deist, T.M., Peerlings, J., de Jong, E.E.C., van Timmeren, J., Sanduleanu, S., Larue, R.T.H.M., Even, A.J.G., Jochems, A., et al. (2017). Radiomics: the bridge between medical imaging and personalized medicine. Nat. Rev. Clin. Oncol. *14*, 749–762.
9. Dong, D., Fang, M.J., Tang, L., Shan, X.H., Gao, J.B., Giganti, F., Wang, R.P., Chen, X., Wang, X.X., Palumbo, D., et al. (2020). Deep learning radiomic nomogram can predict the number of lymph node metastasis in locally advanced gastric cancer: an international multicenter study. Ann. Oncol. *31*, 912–920.
10. Fink, C., Baumann, P., Wente, M.N., Knebel, P., Bruckner, T., Ulrich, A., Werner, J., Büchler, M.W., and Diener, M.K. (2014). Incisional hernia rate 3 years after midline laparotomy. Br. J. Surg. *101*, 51–54.
11. Burger, J.W.A., Luijendijk, R.W., Hop, W.C.J., Halm, J.A., Verdaasdonk, E.G.G., and Jeekel, J. (2004). Long-term follow-up of a randomized controlled trial of suture versus mesh repair of incisional hernia. Ann. Surg. *240*, 578–585.
12. Lambrichts, D.P.V., de Smet, G.H.J., van der Bogt, R.D., Kroese, L.F., Menon, A.G., Jeekel, J., Kleinrensink, G.J., and Lange, J.F. (2018). Incidence, risk factors and prevention of stoma site incisional hernias: a systematic review and meta-analysis. Colorectal Dis. *20*, O288–O303.
13. Bhangu, A., Fletcher, L., Kingdon, S., Smith, E., Nepogodiev, D., and Janjua, U. (2012). A clinical and radiological assessment of incisional hernias following closure of temporary stomas. Surgeon *10*, 321–325.
14. Oriel, B.S., Chen, Q., and Itani, K.M.F. (2017). Incidence, recurrence and risk factors of hernias following stoma reversal. Am. J. Surg. *214*, 232–238.
15. Hou, H., Chen, D., Zhang, K., Zhang, W., Liu, T., Wang, S., Dai, X., Wang, B., Zhong, W., and Cao, H. (2022). Gut microbiota-derived short-chain fatty acids and colorectal cancer: Ready for clinical translation? Cancer Lett. *526*, 225–235.
16. Lorenz, A., Kogler, P., Kafka-Ritsch, R., Öfner, D., and Perathoner, A. (2019). Incisional hernia at the site of stoma reversal-incidence and risk factors in a retrospective observational analysis. Int. J. Colorectal Dis. *34*, 1179–1187.
17. Meng, L., Dong, D., Chen, X., Fang, M., Wang, R., Li, J., Liu, Z., and Tian, J. (2021). 2D and 3D CT Radiomic Features Performance Comparison in Characterization of Gastric Cancer: A Multi-Center Study. IEEE J. Biomed. Health Inform. *25*, 755–763.

STAR★METHODS

KEY RESOURCES TABLE

REAGENT or RESOURCE	SOURCE	IDENTIFIER
Deposited data		
Clinical data and CT images	Shanghai Jiaotong University, Renji Hospital	N/A
	Fudan University, Huadong Hospital	N/A
Software and algorithms		
Python	Python software	https://www.python.org/
Rstudio	R software	https://rstudio.com/products/rstudio/
ITK-SNAP	ITK-SNAP (version 3.8.0)	http://www.itksnap.org/pmwiki/pmwiki.php
Mendeley Data		https://doi.org/10.17632/pm36fhmxyr.1

EXPERIMENTAL MODEL AND STUDY PARTICIPANT DETAILS

We collected CT images of prophylactic terminal ileostomy performed at Renji Hospital, Shanghai Jiao Tong University and Huadong Hospital, Fudan University. Search for the keywords "colorectal cancer" and "ileostomy" in the electronic medical records system. These SSIH cases at the two hospitals were diagnosed between January 2017 and May 2018. In external validation cohort 2, we included patients with non-colorectal cancer ostomy from Renji Hospital. We excluded patients who had no plain CT or only enhanced CT scan prior to ostomy closure. Meanwhile, patients who had no regular follow-up after ostomy restoration are also excluded. The detailed flow of the dataset is shown in Figure 1. Details of the study participants are shown in Tables 1 and S1. The data is not available and only the image file is used.

This retrospective study was approved by the Shanghai Jiaotong University School of Medicine, Renji Hospital Ethics Committee (No. KY2022-087-B) and informed consent was obtained from patients.

METHOD DETAILS

Patients and datasets

All patients were enrolled if they met all the inclusion criteria and were excluded if they met at least one of the following exclusion criteria. The inclusion criteria were as follows: (1) age $\geq$18 years, (2) accepted curative resection of colorectal cancer (primary cohort and external cohort 1), prophylactic ileostomy + stoma closure operation (all cohorts), (3) complete clinical information and imaging data, and (4) diagnosis of SSIH within one year postoperatively. The exclusion criteria were as follows: (1) no imaging examination performed before the stoma closure operation, (2) follow-up time of less than one year or loss, and (3) other abdominal operations performed during the study period. For patients undergoing routine review in Renji or Huadong hospital, SSIH was determined by physical examination and CT imaging diagnosis. For patients in other hospitals, the patient's medical records including physical examination and CT scan results were obtained through telephone follow-up.[4]

Eligible patients were enrolled from two centers in China and divided into four cohorts: a training cohort, an internal validation cohort, external cohort 1, and external cohort 2 (Non-tumor patients: Patients with terminal ileostomy due to inflammatory bowel disease, intestinal perforation or trauma). The training cohort was used to construct the mixed model. The internal validation cohort and external cohort 1 were used to test the validity of the model in colorectal cancer patients, and external cohort 2 was used to test the validity in patients with ostomies for other reasons. The modeling pipeline is illustrated in Figure 2.

Radiomics and clinical features extraction

The clinical characteristics of the patients are shown in Table 1. Parastomal hernia, distance from the anal margin, and *trans*-or lateral rectus abdominis (stoma) were determined by experienced radiologists based on preoperative CT images. The T and N stages were determined using pathological findings as the gold standard. Other data were collected by reviewing patients' medical records.

All patients underwent abdominopelvic CT before stoma closure. The regions of interest (ROIs) were manually delineated on the CT images by two experienced radiologists using the ITK-SNAP software (version 3.8.0; http://www.itksnap.org). In principle, only the slide with the widest separation from the abdominal wall was visually chosen to delineate the muscle and soft tissue regions. For all ROIs, the medial boundary was the medioventral line, and the lateral boundary was set by the midaxillary line. When disagreements arose, a third reviewer made the final decision. After three months, 30 patients were randomly selected, and the ROIs were delineated by two additional radiologists. The dataset was used to assess the reproducibility of intra-and internal reader radiomics features.

All images were resampled using Python (3.7.1) to isotropic voxels of 1 × 1 × 1 mm^3 before radiomic feature extraction using the B-spline interpolation function in the SimpleITK package (2.1.1.2). Quantitative radiomics features (first-order, shape, texture, wavelet, and Laplacian of

the Gaussian filter) were extracted from these ROIs using the open-source Pyradiomics package (Version 2.1.1). We extracted 1316 radiomic features (32 first-order statistical features, 75 texture features, and 1209 wavelet and log decompositions) from each ROI.

Architecture of radiomics models

Feature selection and signature building were performed using the Renji cohort. The radiomic model was built according to the following steps: (1) the intra-and inter-class correlation coefficients (ICCs) were calculated based on the re-segmentation dataset, and features with ICCs<0.75 were removed. (2) Spearman's correlation analysis was used to analyze the correlation of the remaining features, and if the correlation coefficient between two features was greater than 0.9, only one of the features was retained, (3) the least absolute shrinkage and selection operator (LASSO) logistic regression algorithm, 20 with penalty parameter tuning conducted by 10-fold cross-validation, was then applied to select the SSIH-related features, (5) three models, support vector machine (SVM), artificial neural network (ANN), and random forest (RF), were constructed based on features whose absolute coefficient values were greater than 0.015, and (6) based on the accuracy of the model, we assigned a weight to each model. The three models were combined into a final mixed model based on their respective weights. The Kolmogorov-Smirnov test was used to determine the best threshold for the mixed model to achieve the best predictive power.

Deep learning image processing

In contrast to the original MobileNet, the MobileNetV2 architecture is based on an inverted residual block with thin bottleneck layers. It uses the expansion layer to expand the dimension, lightweight depthwise convolutions to filter features, and finally the projection layer to compress the data, which has the effect of drastically reducing the computation and model size. After standardization, all images with a size of 224 × 224 pixels and three color channels were input into the model. Approximately 60% of the randomly selected data were used as a training set and enhanced by methods such as horizontal shifting. The batch size of the model was set to 8.

Owing to the size of the data, transfer learning helps to directly obtain the official network model architecture that has been built, and the trained weight parameters are applied to the model. Starting with a MobileNetV2 model based on ImageNet-trained weights, there were 154 layers in this network. The first 120 layers, including the weight parameters, were frozen, whereas the rest could be changed to optimize the network. A flattened and a fully connected layer (FC) were added to flatten the output results and perform feature extraction. The dropout layer was designed to prevent overfitting so that the neurons could be removed from the network with 50% probability. Finally, the softmax function was used to predict the results of binary classification.

Models

To train the model sufficiently, focal loss was chosen as the loss function to solve the class imbalance. Exponential decay was applied in the process. Before each epoch, the learning rate was reset to the initial learning rate of 0.0001, and then the decay started again, while the decay step and rate were set to 50 and 0.96, respectively. The accuracy, loss and areas under the curve (AUC) of the training and validation set would be output as metrics. EarlyStopping, based on val loss, was also added to prevent overfitting. The AUC of the mixed deep learning, radiomics, and clinical models were compared for all cohorts. Multiple comparisons of the ROCs were performed using the DeLong test. A confusion matrix was used to describe the overall performance. Decision curve analysis was conducted to evaluate the clinical practicability and net benefits of the mixed model in predicting high-risk patients with SSIH. We further validated our mixed model in Huadong colorectal cancer (external cohort 1) and non-tumor patients who underwent stoma closure (external cohort 2) using the AUC and confusion matrix.

QUANTIFICATION AND STATISTICAL ANALYSIS

Statistical significance was set at $p < 0.05$ (two-sided). We compared two groups using the t-test for continuous variables and the chi-square test or Fisher's exact test for categorical variables. Stepwise regression models were used to estimate the odds ratio (OR) and 95% confidence interval (CI) and to identify independent prognostic clinical variables for SSIH in the primary cohort. Logistic regression coefficients were used to generate mixed models and nomograms.